Large-scale reorganization of the tonotopic map in mouse auditory midbrain revealed by MRI

Xin Yu*†‡, Dan H. Sanes§, Orlando Aristizabal*†, Youssef Zaim Wadghiri†, and Daniel H. Turnbull*†‡¶‖

*Skirball Institute of Biomolecular Medicine, Departments of †Radiology and ¶Pathology, and ‡Graduate Program in Neuroscience and Physiology, New York University School of Medicine, New York, NY 10016; and §Center for Neural Science, New York University, NY 10003

Edited by Eric I. Knudsen, Stanford University School of Medicine, Stanford, CA, and approved June 7, 2007 (received for review February 1, 2007)

The cortex is thought to be the primary site of sensory plasticity, particularly during development. Here, we report that large-scale reorganization of the mouse auditory midbrain tonotopic map is induced by a specific sound-rearing environment consisting of paired low- (16 kHz) and high-frequency (40 kHz) tones. To determine the potential for plasticity in the mouse auditory midbrain, we used manganese-enhanced MRI to analyze the midbrain tonotopic maps of control mice during normal development and mice reared in the two-tone (16 + 40 kHz) environment. We found that the tonotopic map emerged during the third postnatal week in normal mice. Before 3 weeks, a larger percentage of auditory midbrain responded to each of the suprathreshold test frequencies, despite the fact that the primary afferent projections are in place even before hearing onset. By 3 weeks, the midbrain tonotopic map of control mice was established, and manganese-enhanced MRI showed a clear separation between the 16- and 40-kHz responses. Two-tone rearing dramatically altered the appearance of these discrete frequency-specific responses. A significant volume of the auditory midbrain became responsive to both rearing frequencies, resulting in a large-scale reorganization of the tonotopic map. These results indicate that developmental plasticity occurs on a much greater scale than previously appreciated in the mammalian auditory midbrain.

developmental plasticity | inferior colliculus | neuroimaging | manganese | sound rearing

The sensory cortices are thought to be primary sites of long-term plasticity, particularly during critical early periods of mammalian brain development. Previous studies have shown that the rearing environment profoundly influences neuronal coding properties recorded in the visual, auditory, somatosensory, and olfactory cortices (1–9). In the central auditory pathway, most ascending projections from the lower brainstem nuclei terminate in the inferior colliculus (IC), and this structure is the principal conduit of ascending projections to the thalamus. Given the tremendous convergence of ascending afferents to the IC, it is possible that this area serves as a primary site of developmental plasticity. In fact, experimental manipulations on developing barn owls reveal an activity-dependent adjustment of binaural coding properties within the IC (10–13). Here, we investigate whether the midbrain is similarly a primary site of developmental plasticity in the mouse auditory system using manganese-enhanced MRI (MEMRI), a new high-resolution neuroimaging method that has been applied for analyzing activity in a number of previous studies (14–19).

Synaptic activity can influence the maturation of neuronal connections in two general ways. It can either serve to stabilize existing connections or progressively induce new connections. An example of the former is the pattern of eye-specific thalamic innervations of visual cortex, where the initial thalamic afferent projection fails to undergo refinement in the absence of appropriate synaptic activity (20–23). An example of the latter is the auditory projection in prism-reared owls, where a new neuronal projection is formed in the IC, adjusting to match the displaced visual activity (13). From these results, it is clear that activity-dependent synaptic plasticity is not confined to the cortical regions but can occur in many subcortical elements of vertebrate brains. However, in the mammalian brain, studies on developmental plasticity have focused largely on the cortex. As a result, the magnitude of subcortical plasticity changes have not been properly evaluated when interpreting experience-dependent behavioral adaptation and learning in mammals.

Critical to our understanding of developmental plasticity is familiarity with the functional status of the system during the period of manipulation (24, 25). In the auditory system, it has been difficult to understand how rearing environments can so dramatically alter sensory coding properties because anatomical studies revealed that topographic afferents project targets well before the onset of hearing (26–29). The present MEMRI study offers a possible resolution to this problem by showing that a large fraction of the immature auditory midbrain responds to single pure tones when presented at sound levels well above threshold. Thus, a wide range of afferents may functionally interact with one another during early postnatal development. Furthermore, our results show a clear reorganization of the mouse midbrain tonotopic map after two-tone rearing, demonstrating developmental plasticity on a much larger scale than previously appreciated and highlighting the importance of analyzing subcortical mammalian brain regions in plasticity experiments.

Results

Pure Tone MEMRI Activity Patterns of the IC. In the past, we reported that MEMRI could be used to detect sound-evoked activity, including activity related to the tonotopic organization in the mouse IC at age 3 weeks (14). Specifically, we demonstrated that MEMRI enhancement patterns became more restricted as the exposure sound bandwidth was decreased. An initial goal of the current study was to quantify MEMRI activity patterns resulting from specific tonal stimuli.

MEMRI enhancement patterns acquired from postnatal day (P) 19 mice exposed to 16 or 40 kHz were each spatially distinct (Fig. 1 *A–F*). Enhancement was restricted to the central region of the IC after 16-kHz stimulation, whereas a clear ventral-caudal band of enhancement was observed after 40-kHz stimulation. To quantify these activity patterns, statistical *p*-maps were generated by voxelwise comparisons of mice exposed to either 16

Author contributions: X.Y., D.H.S., and D.H.T. designed research; X.Y. performed research; O.A. and Y.Z.W. contributed new reagents/analytic tools; X.Y. analyzed data; and X.Y., D.H.S., and D.H.T. wrote the paper.

The authors declare no conflict of interest.

This article is a PNAS Direct Submission.

Freely available online through the PNAS open access option.

Abbreviations: IC, inferior colliculus; MEMRI, manganese-enhanced MRI; ROI, region of interest; SPL, sound pressure level; P*n*, postnatal day *n*.

‖To whom correspondence should be addressed at: Skirball Institute of Biomolecular Medicine, New York University School of Medicine, 540 First Avenue, New York, NY 10016. E-mail: turnbull@saturn.med.nyu.edu.

This article contains supporting information online at www.pnas.org/cgi/content/full/0700960104/DC1.

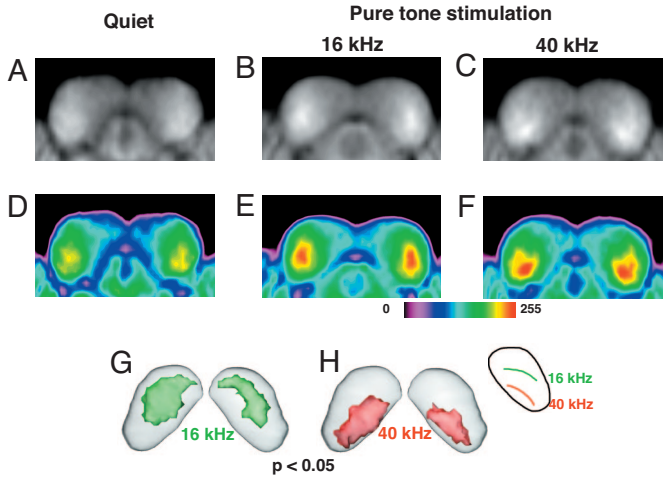

Fig. 1. Pure-tone stimulation induced tonotopic signal enhancement in the IC. Averaged coronal IC images ($n \geq 8$ in each group) demonstrated spatial differences in MEMRI enhancement between mice kept in a quiet environment (*A*) and mice exposed to either 16 kHz (*B*) or 40 kHz (*C*). Pseudocolor-coded images (*D–F*) made it easier to appreciate the enhancement patterns (color scale included). *t*-test analysis, comparing either the 16-kHz-exposed group to the quiet controls (green) (*G*) or the 40-kHz-exposed group to the quiet controls (red) (*H*), shows the regions of significant differences in MEMRI enhancement ($P < 0.05$) in general agreement with the established electrophysiological tonotopic map (*Inset*) (29).

or 40 kHz with mice kept in a quiet environment. The 3D *p*-maps demonstrated significant differences in the IC regions activated by each tone, with the 16-kHz response located centrally and the 40-kHz response located in the ventral-caudal IC [Fig. 1 *G* and *H* and supporting information (SI) Movies 1 and 2; $P < 0.05$]. Furthermore, the dorsal-ventral alignment of the statistically significant regions was in excellent agreement with published electrophysiology maps (30). These results show that MEMRI provides a quantitative and unbiased approach to analyze frequency-dependent activity patterns, induced in the awake mouse IC and imaged subsequently with *in vivo* MRI.

Development of IC Tonotopic Organization. To determine whether the developing nervous system displays a refinement of sound-evoked activity patterns, we compared 16- and 40-kHz-evoked activity patterns at three developmental stages: P13, P16, and P19 (Fig. 2). Sound stimulation was provided at 89 dB [sound pressure level (SPL), peak value] to ensure that the SPL was above the threshold of auditory neurons at the youngest age examined (30). At each stage, images were also acquired from mice kept in a quiet environment to permit statistical comparisons between the magnetic resonance images. At P13, 3 d after the onset of response to airborne sound (30), the activity patterns elicited by each of the two tones were indistinguishable (Fig. 2 *A* and *B*). At P16, signal-enhancement patterns between the two tones began to exhibit separate loci. Statistical analysis indicated that the 16 kHz tone-activated signal enhancement was shifted dorsally compared with the 40-kHz activity pattern (Fig. 2 *A* and *B*). By P19, the activity patterns evoked by each tone were clearly separated. Statistical *p*-maps showed that the pattern of IC activity evoked by a 40-kHz pure tone resolved into the expected ventrocaudal contour, whereas the pattern evoked by a 16-kHz pure tone was located in a more dorsal and central region of the IC (Fig. 2 *A* and *B*). Quantitative analysis revealed that the percent overlap of the 16- and 40-kHz-responsive regions declined from 72% at P13 to 17% at P19 (Fig. 2*C*), and the centroid-to-centroid separation between the 16- and 40-kHz activity regions increased from 200 μm at P13 to 600 μm at P19 (Fig. 2*D*). These results characterize the maturation of sound-activated regions of IC during normal auditory brain development. Specifically, they demonstrate that suprathreshold tonal stimuli activate a large percentage of the IC close to the time of hearing onset. Furthermore, they demonstrate that dissimilar sounds can coactivate the same IC regions when coadministered during this period of development.

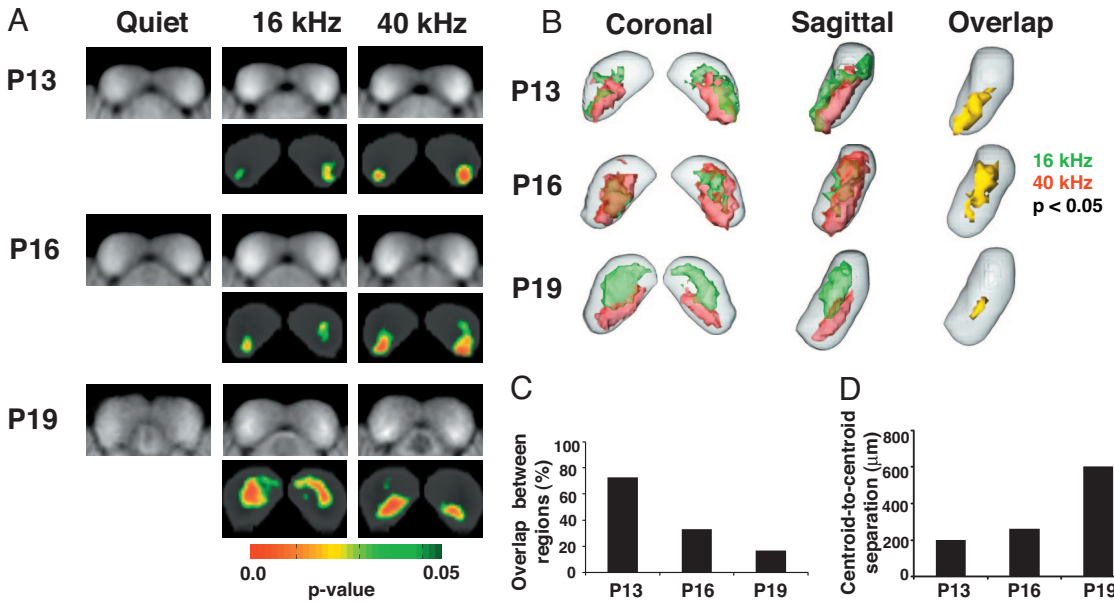

Fig. 2. Volumetric analysis is used to quantify the developmental differences in activity. (*A*) MEMRI 2D coronal images and 2D *p*-maps show the developmental changes in tone-induced activity (color scale for *p*-maps is shown). (*B*) Three-dimensional *p*-maps ($P < 0.05$) show the 16-kHz (green) and 40-kHz (red) activity patterns at P13 (*Top*), P16 (*Middle*), and P19 (*Bottom*). At each stage, the 3D *p*-maps are displayed in both coronal (*Left*) and sagittal (*Center*) views. The region of overlap between 16 and 40 kHz (yellow) (*Right*) is also shown for each postnatal age. Quantitative analysis demonstrated a decrease in the overlap volume (*C*) and an increase in the centroid-to-centroid separation (*D*) with increasing developmental stage.

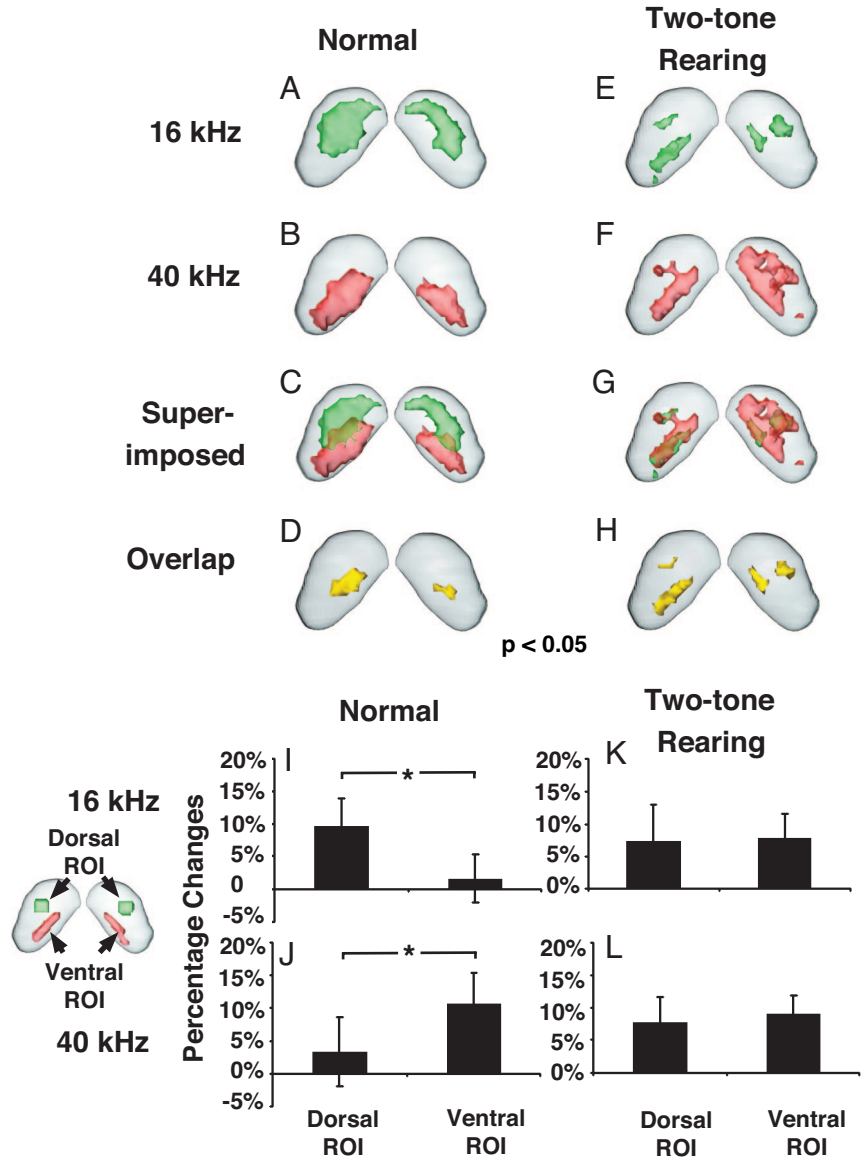

Fig. 3. Two-tone (16 + 40 kHz) rearing induced changes in both the 16- and 40-kHz IC activity patterns. Three-dimensional *p*-maps of normal (*A–D*) and two-tone-reared mice (*E–H*) demonstrate marked differences in both the 16-kHz (green) (*A* and *E*) and 40-kHz (red) (*B* and *F*) activity patterns ($P < 0.05$; $n \geq 8$ in each group). The superimposed activity maps show differences in overlap (yellow) between 16- and 40-kHz patterns in two-tone-reared mice (*G* and *H*) compared with normal controls (*C* and *D*). In two-tone-reared mice, the regions of overlap between the 16- and 40-kHz patterns (yellow) (*H*) clearly separate the altered distribution into dorsal (putative 16 kHz) and ventral (putative 40 kHz) IC. (*I–L*) Quantitative ROI analysis (dorsal ROI, green; ventral ROI, red) (*Inset*) shows significant differences between dorsal and ventral MEMRI signal enhancement in normal mice at both 16-kHz (*I*) and 40-kHz (*J*) (*, $P < 0.01$). In contrast, the two-tone-reared mice show no dorsal–ventral differences at either 16 kHz (*K*) or 40 kHz (*L*).

Acoustic Manipulation During Early Auditory Brain Development. To examine experience-dependent plasticity in the IC, we reared neonatal mice in a synchronous two-tone (16 + 40 kHz) acoustic environment during the period when distinct spatial activity patterns were emerging (P9–P17). Two-tone-reared mice were then kept in a silent environment for 24 h and tonotopicity was assessed with either a 16- or 40-kHz stimulation. As with previous experiments, the activity patterns were analyzed statistically by comparing images from stimulated animals with images from mice kept in a quiet environment. After 16 + 40 kHz rearing, the MEMRI *p*-maps showed overlapping activity regions corresponding to the 16- and 40-kHz-frequency coding areas (Fig. 3 *A–H*). Regions of interest (ROIs) were chosen within the center response region for each frequency in normal mice and the enhanced dorsal and ventral regions in two-tone-reared mice. Quantitative analysis in these dorsal and ventral ROIs showed significant differences between 16- and 40-kHz MEMRI intensity in normal mice, as expected, but no differences in two-tone-reared mice (Fig. 3 *I–L*). These markedly different activity patterns demonstrate that the rearing environment induced aberrant functional responses and/or connections in the IC of the two-tone-reared mice.

Although the 16- and 40-kHz spatial patterns were clearly altered in the two-tone-reared mice, it was not clear whether the effect was limited to the rearing tones or whether the entire IC tonotopic organization had been altered. Therefore, we examined the activity pattern of a third frequency (32 kHz) in control and two-tone-reared mice. The 32-kHz coding area in the mice reared in the normal condition was located between the 16- and 40-kHz coding regions, in excellent agreement with the tonotopic map established

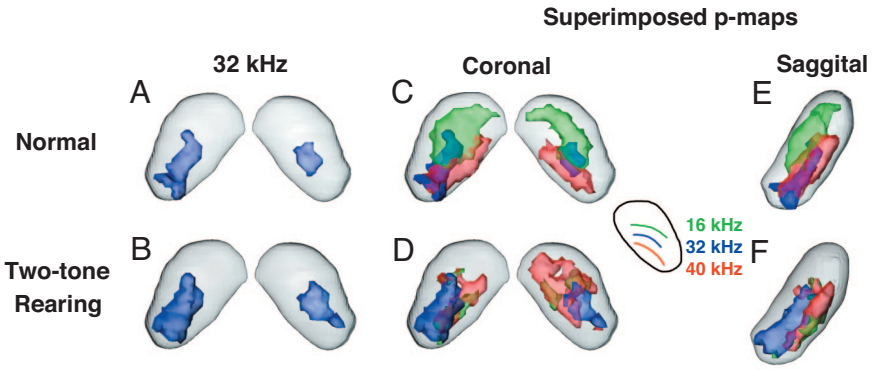

Fig. 4. The changes in IC activity patterns were specific to the rearing tones. Similar activity patterns (blue) were observed after 32-kHz stimulation of normal (*A*) ($P < 0.05$, $n \geq 8$) and two-tone-reared mice (*B*) ($P < 0.05$, $n \geq 8$). Superimposed *p*-maps ($P < 0.05$; $n \geq 8$ in each group) show the relative positions of the 16-kHz (green), 32-kHz (blue), and 40-kHz (red) activity patterns in normal (*C* and *E*) and two-tone-reared mice (*D* and *F*). The corresponding electrophysiological tonotopic map is also shown for reference (*Inset*).

by electrophysiology (30). A similar pattern of 32-kHz-evoked activity was observed in the two-tone-reared mice (Fig. 4), indicating that the effect of two-tone rearing was specific to afferent activity recruited by 16 and 40 kHz.

Discussion

In the present study, MEMRI was used to analyze the early development of the midbrain response to suprathreshold tonal stimuli. At P19, the 3D activity patterns associated with each sound frequency were aligned tonotopically in the IC, in good agreement with the spatial organization of tonotopic maps established by electrophysiology (30). In contrast, at P13 and P16, the activity patterns were largely overlapping, indicating that single IC neurons are likely responsive to multiple frequencies at early developmental stages. Furthermore, the tone-evoked activity patterns were profoundly altered in mice reared in an environment consisting of paired low- and high-frequency tones. This study establishes that environmental manipulations produce large-scale functional alterations in the mammalian auditory midbrain (Fig. 3).

In the current experiments, there was unavoidable variability in SPLs experienced by the free-ranging mice during both the rearing and stimulation periods. In addition, there are inherent differences in acoustic energy carried by the amplitude-modulated single-tone (stimulation) and two-tone (rearing) waveforms. Notwithstanding these complications in the experimental design, the resulting response patterns in control animals during the period of manipulation (Fig. 2) suggest that the rearing stimuli likely coactive a large fraction of the IC.

Studies have shown that the primary afferent projections in the auditory brainstem and IC develop before the onset of hearing (26, 28, 31, 32). In contrast, intracellular studies tend to show that functional characteristics, including long-term synaptic plasticity, continue to mature well after this period (33, 34). Thus, it is possible that changes to synaptic efficacy could alter single-neuron coding properties even in the absence of changes in connectivity. It has been found that repetitive acoustic stimulation (pulsed white noise or clicks) can alter coding properties after the afferent connectivity has been established (5, 25, 35). Such repetitive environmental noise deprived the animals of the normal patterned environmental acoustic inputs (24) and resulted in disrupted tonotopy and degraded neuronal response selectivity. Studies focusing on tone exposure during early postnatal stages showed expansion of the receptive field for the exposed tone frequency in the primary auditory cortex (4) and increased the number of auditory neurons with a low threshold response to the exposed tone-frequencies in the IC (25, 36). Single neurons in the mouse IC display discrete responses to more than one frequency, and the efficacy of these bimodal responses may be enhanced by two-tone rearing (24). Our current results provide data on normal-tone-evoked activity patterns during the rearing period itself.

Our results indicate that concurrent activation of afferents responding to 16 or 40 kHz leads to an alteration of functional connectivity that should provide strong motivation for future anatomical studies. The basis for this plasticity might involve the rewiring of 16- and 40-kHz afferent projections, although this seems unlikely because these projections are formed early in development and are well separated spatially. Alternatively, there might be an increase of convergent excitatory inputs (i.e., inputs with different characteristic frequencies) to neurons within lower auditory brainstem nuclei that send excitatory projections to the IC. In this scenario, IC neurons would inherit broader tuning from their afferents. Finally, the observed changes could result from an increase of convergent excitatory projections (local, ascending, or descending) or a decrease in inhibitory projections (local, ascending or descending) to IC neurons between the 16- and 40-kHz domains. For example, the local axonal projections of IC neurons could establish and strengthen connections within or across the fibrodendritic laminae in the central nucleus of the IC during development (37). Recordings of disynaptic currents in IC neurons have suggested that local IC neurons are coupled together to function during the acoustic information processing (38). The synchronous two-tone inputs may therefore modify the secondary synaptic inputs between the neurons located in the 16- and 40-kHz-sensitive regions in the P19 mice. This strengthened excitatory disynaptic input could then result in the two-frequency-activated regions we observed after stimulation with either 16 or 40 kHz, whereas the weakened inhibitory disynaptic input could function to increase the size of the activated regions (Fig. 3). In fact, a dramatic reduction of inhibitory strength within the IC has been shown to occur in a use-dependent fashion (39).

It is now clear that the acoustic environment can dramatically alter the frequency-response properties, as assessed by recordings from both the IC and the auditory cortex (4, 5, 25, 36, 40). Because these structures are functionally coupled through both ascending and descending projections, it remains unknown whether one or both loci are the primary sites of plasticity. Given that numerous examples of subcortical developmental plasticity have been observed in lower vertebrates, from *Xenopus* to avian species (11, 13, 41, 42), it is unlikely that the altered activity patterns we have demonstrated in the mouse auditory midbrain are solely dependent on changes in the auditory cortex. How-

ever, an important future goal should be to identify the primary source(s) of these functional changes in the mammalian auditory system and to determine the relationship between changes in the IC, thalamus, and cortex.

In a broader context, our results highlight the importance of whole-brain analysis in understanding plasticity in the developing mammalian brain. Although previous rearing studies have focused almost exclusively on cortical plasticity, our results demonstrate that rearing can alter the signal processing in the IC, a major subcortical nucleus of the central auditory system. This study clearly demonstrates that MEMRI both provides a global view of the neuronal activity in the mature mouse brain and enables analysis of the refinement of activity patterns in the developing mouse brain. Importantly, the spatial activity information provided by MEMRI can be used in the future to guide further investigations of the firing properties of individual neurons and the projections of the targeted neuronal circuits. Finally, the ability to map activity in the developing mouse IC will provide a powerful tool for future analysis of functional phenotypes in genetically engineered mouse models with developmental midbrain defects.

Methods

Animal Preparation. The mice used in this study were maintained under protocols approved by the Institutional Animal Care and Use Committee of New York University School of Medicine. The procedure to prepare mice for MEMRI was similar to that used in other studies (14, 43). Mice from the Institute of Cancer Research (ICR) were injected i.p. with $MnCl_2$ (0.4 mmol/kg) at stages ranging from P12 to P18. After injection, mice were immediately exposed to defined sound stimuli (see below) or kept in a quiet acoustic environment for 24 h.

As shown previously, MEMRI provides an effective method for mapping accumulated auditory brain activity in awake, normal-behaving mice (14). During sound exposure or quiet, mice were maintained under normal living conditions with a 12-h-light/12-h-dark cycle and free access to food and water. Mice were awake during the acoustic stimulation that produces each pattern of Mn accumulation and were imaged subsequently in the anesthetized state. Preweaning-stage mouse pups were kept together with the mother. Neither Mn administration nor sound stimulation induced abnormal behavior during the 24-h time period. In this study, we imaged a total of 120 mice, of which 107 (89%) were used in the final analyses. Of the 13 mice that were not used, 3 died during anesthesia/MRI, 4 had unacceptable motion artifacts, and 6 were noticeably hypoxic, resulting in unacceptable artifacts caused by deoxygenated blood.

Acoustic Stimulation. Acoustic waveforms were generated on a programmable function/arbitrary waveform generator (model 33220A; Agilent Technologies, Palo Alto, CA), amplified with a high-fidelity audio amplifier (XPLORE model AMP-4030), and delivered through an audio speaker (Vifa model XT25TG30). The speaker was mounted inside an acoustic isolation chamber [Industrial Acoustics (Bronx, NY) model Mac-1] lined with polyurethane anechoic wedge panels (Acoustics First, Richmond, VA). Mice were kept in standard mouse microisolator cages placed within the acoustic chamber during the 24-h period of sound exposure or quiet (control). The amplitude and spectral characteristics of the sound stimuli, as well as the noise floor, were measured with a multichannel spectrum analyzer [Bruel & Kjaer (Norcross, GA) model 3550] by using a quarter-inch free-field condenser microphone. The system was calibrated with a model 4294 (Bruel & Kjaer) vibration reference source.

Sound stimulation consisted of single tones (16, 32, and 40 kHz) or a synchronous two-tone stimulus (16 + 40 kHz). The amplitudes of the carriers were modulated at 4 Hz with a modulation depth of 90%. The amplitude modulation was implemented in an attempt to avoid habituation of the IC neurons to the repetitive stimuli (14). For all experiments except the two-tone rearing protocol, the amplitude-modulated stimuli had a peak SPL of 89 dB. This SPL was chosen after determining the response to three different sound levels (14). It should be noted that due to the geometries of the acoustic chamber, the mouse cage, and the microphone, the calibration point was placed in the center of the cage and ≈10 cm above the bottom level where the mice resided during most of the stimulation and rearing periods. Because of the variable positions of the mice in the cage and the fact that their ears were sometimes facing away from the speaker, the calibrated peak amplitudes reported here (89 dB SPL for stimulation; 77 dB SPL for rearing) could be significantly higher than the levels actually experienced by the mice.

Two-Tone Rearing. Neonatal mice were exposed to a synchronous two-tone stimulus (16 + 40 kHz, 77dB SPL, peak value) from P9 through P17. This SPL was chosen to ensure that a significant response would be elicited in even the youngest animals, where thresholds are known to be high. Because the peak amplitudes of both tones in the stimulation waveform were 77dB SPL, the actual (calibrated) sound pressure of the combined rearing signal was actually 3 dB greater than 77 dB SPL. As noted in the previous section, this quoted SPL is the calibrated peak value at the reference point above the cage bottom. The actual SPLs experienced by the mice will depend on their (variable) positions in the cages over the 9-d rearing period. During the rearing period, mice were exposed to the sound stimulation for 22–23 h/d and were in the normal cage room environment for the remaining 1–2 h/d to accommodate veterinary health monitoring. At P17, the two-tone-reared mice were kept in a quiet environment for 24 h. $MnCl_2$ was injected at P18 and the animals were exposed to a specific tone stimulus (16, 32, or 40 kHz) for 24 h. MRI images were acquired at P19 immediately after the sound exposure. Control studies were performed on mice maintained under normal rearing conditions.

MRI Data Acquisition. MRI was performed on a microimaging system (Surrey Medical Imaging Systems, Guildford, U.K.) consisting of a 7-T horizontal magnet (Magnex Scientific, Palo Alto, CA) with actively shielded gradients (Magnex Scientific; 250 mT/m gradient strength, 200-μs rise time) and a 25-mm (inner diameter) quadrature Litz mouse head coil (Doty Scientific, Columbia, SC). The coil was incorporated into a custom holder with a tooth bar to immobilize the head and a nose cone for isoflurane gas delivery with an anesthesia machine (VMS; Matrix Medical, Orchard Park, NY). T1-weighted brain images were acquired with a 3D gradient echo pulse sequence [echo time (TE) = 4 ms, repetition time (TR) = 50 ms, flip angle = 65°], resulting in a volumetric image set covering the entire brain, with isotropic spatial resolution of 100 μm in a total imaging time of 110 min per mouse.

Image Processing and Statistical Analysis. Briefly, volumetric magnetic resonance image data were processed with Amira (version 3.1; Mercury Computer Systems–TGS, Chelmsford, MA) to segment and register each mouse brain to a 3D template, created by averaging 13 registered whole-brain images. To reduce the image-to-image signal differences produced by MRI acquisition variability, the histograms were normalized, resulting in 3D whole-brain images with equal mean and standard deviation. The IC was extracted from each mouse brain in Amira by using an IC mask segmented from the whole-brain template. Image processing was performed separately at each developmental stage, creating different IC masks at P13, P16, and P19.

To represent the patterns of sound-evoked signal enhancement in the auditory midbrain, 3D images of the IC were analyzed statistically with a voxelwise multiple-comparison method implemented in MATLAB (version 7.1; MathWorks, Natick, MA). Student's *t* tests (two-tailed) were performed between equivalent voxels in sound-stimulated IC images and quiet control IC images. The resulting *P* value was assigned to each voxel to create a 3D statistical map, which was smoothed by convolution with a Gaussian filter kernel ($3 \times 3 \times 3$). The statistical maps were displayed as color-coded 2D slices or as 3D volumetric surface contours after threshold detection ($P < 0.05$).

We thank Drs. James Babb, Glyn Johnson, and Jing Zou for advice on the statistics and image analysis; Jeffrey and Raymond Blind for designing and fabricating the mouse holder used in these experiments; and Drs. Gord Fishell and Wen-biao Gan for critical review of this work. This work was supported by National Institutes of Health Grants NS038461 (to D.H.T.), DC006892 (to D.H.T.), and DC006864 (to D.H.S.).

1. Blakemore C, Cooper GF (1970) *Nature* 228:477–478.
2. Stryker MP, Sherk H (1975) *Science* 190:904–906.
3. Hirsch HV, Spinelli DN (1970) *Science* 168:869–871.
4. Zhang LI, Bao S, Merzenich MM (2001) *Nat Neurosci* 4:1123–1130.
5. Zhang LI, Bao S, Merzenich MM (2002) *Proc Natl Acad Sci USA* 99:2309–2314.
6. Seo ML (1992) *Dev Psychobiol* 25:67–76.
7. Fox KA (1992) *J Neurosci* 9:1128-l 135.
8. Polley DB, Kvasnak E, Frostig RD (2004) *Nature* 429:67–71.
9. Franks KM, Isaacson JS (2005) *Neuron* 47:101–114.
10. Brainard MS, Knudsen EI (1993) *J Neurosci* 13:4589–4608.
11. Knudsen EI (1998) *Science* 279:1531–1533.
12. Zheng W, Knudsen EI (1999) *Science* 284:962–965.
13. DeBello WM, Feldman DE, Knudsen EI (2001) *J Neurosci* 21:3161–3174.
14. Yu X, Wadghiri YZ, Sanes DH, Turnbull DH (2005) *Nat Neurosci* 8:961–968.
15. Lin YJ, Koretsky AP (1997) *Magn Reson Med* 38:378–388.
16. Pautler RG, Silva AC, Koretsky AP (1998) *Magn Reson Med* 40:740–748.
17. Kuo YT, Herlihy AH, So PW, Bell JD (2006) *NMR Biomed* 19:1028–1034.
18. Aoki I, Ebisu T, tanka C, Katsuta K, Fujikawa A (2003) *Magn Reson Med* 50:7–12.
19. Berkowitz BA, Roberts R, Goebel DJ, Luan H (2006) *Invest Ophthalmol Vis Sci* 47:2668–2674.
20. Wiesel TN, Hubel DH (1965) *J Neurophysiol* 28:1029–1040.
21. Hubel DH, Wiesel TN (1970) *J Physiol (London)* 206:419–436.
22. Antonini A, Stryker MP (1996) *J Comp Neurol* 369:64–82.
23. Catalano SM, Shatz CJ (1998) *Science* 281:559–562.
24. Sanes DH, Constantine-Paton M (1985) *Brain Res* 354:255–267.
25. Sanes DH, Constantine-Paton M (1985) *J Neurosci* 5:1152–1166.
26. Young SR, Rubel EW (1986) *J Comp Neurol* 254:425–459.
27. Sanes DH, Siverls V (1991) *J Neurobiol* 22:837–854.
28. Leake PA, Snyder RL, Hradek GT (2002) *J Comp Neurol* 448:6–27.
29. Gurung B, Fritzsch B (2004) *J Comp Neurol* 479:309–327.
30. Romand R, Ehret G (1990) *Brain Res Dev Brain Res* 54:221–234.
31. Pienkowski M, Harrison RV (2005) *J Comp Neurol* 492:101–109.
32. Gonzalez-Hernandez TH, Meyer G, Ferres-Torres R (1989) *Neuroscience* 30:127–141.
33. Sanes DH (1993) *J Neurosci* 13:2627–2637.
34. Kotak VC, Sanes DH (2000) *J Neurosci* 20:5820–5826.
35. Oliver DL, Kuwada S, Yin TC, Haberly LB, Henkel CK (1991) *J Comp Neurol* 303:75–100.
36. Poon PW, Chen X (1992) *Brain Res* 585:391–394.
37. Oliver DL, Kuwada S, Yin TC, Haberly LB, Henkel CK (1991) *J Comp Neurol* 303:75–100.
38. Moore DR, Kotak VC, Sanes DH (1998) *J Neurophysiol* 80:2229–2236.
39. Vale C, Sanes DH (2000) *J Neurosci* 20:1912–1921.
40. De Villers-Sidani E, Chang EF, Bao S, Merzenich MM (2007) *J Neurosci* 27:180–189.
41. Udin SB (1983) *Nature* 301:336–338.
42. Fosser NS, Brusco A, Rios H (2005) *Brain Res Dev Brain Res* 160:211–218.
43. Wadghiri YZ, Blind JA, Duan X, Moreno C, Yu X, Joyner AL, Turnbull DH (2004) *NMR Biomed* 17:613–619.